Kinematic Analysis of Dimensional Variation Propagation for Multistage Machining Processes With General Fixture Layouts

Jean-Philippe Loose, Shiyu Zhou, and Dariusz Ceglarek

***Abstract*—Recently, the modeling of variation propagation in complex multistage manufacturing processes has drawn significant attention. In this paper, a linear model is developed to describe the dimensional variation propagation of machining processes through kinematic analysis of the relationships among fixture error, datum error, machine geometric error, and the dimensional quality of the product. The developed modeling technique can handle general fixture layouts rather than being limited to a 3-2-1 layout case. The dimensional error accumulation and transformation within the multistage process are quantitatively described in this model. A systematic procedure to build the model is presented and validated. This model has great potential to be applied toward fault diagnosis and process design evaluation for complex machining processes.**

***Note to Practitioners*—Variation reduction is essential to improve process efficiency and product quality in order to gain a competitive advantage in manufacturing. Unfortunately, variation reduction presents difficult challenges, particularly for large-scale modern manufacturing processes. Due to the increasing complexity of products, modern manufacturing processes often involve multiple stations or operations. For example, multiple setups and operations are often needed in machining processes to finish the final product. When the workpiece passes through multiple stages, machining errors at each stage will be accumulated onto the workpiece and could further influence the subsequent operations. The variation accumulation and propagation pose significant challenges to final product variation analysis and reduction. This paper focuses on a systematic technique for the modeling of dimensional variation propagation in multistage machining processes. The relationship between typical process faults and product quality characteristics are established through a kinematics analysis. One salient feature of the proposed technique is that the interactions among different operations with general fixture layouts are captured systematically through the modeling of setup errors. This model has great potential to be applied to fault diagnosis and process design evaluation for a complex machining process.**

***Index Terms*—Dimensional errors, kinematic analysis, multistage machining processes, variation propagation.**

Manuscript received December 21, 2004; revised October 16, 2005. This work was supported in part by the National Science Foundation award DMI-033147, in part by the Department of Energy, in part by the NIST Advanced Technology Program (ATP Cooperative Agreement 70NANB3H3054), and by industries. This paper was recommended for publication by Associate Editor M. Lawley and Editor P. Ferreira upon evaluation of the reviwers' comments.

The authors are with the Department of Industrial and Systems Engineering, University of Wisconsin, Madison, WI 53706 USA (e-mail: jploose@wisc.edu; szhou@engr.wisc.edu; darek@engr.wisc.edu).

Digital Object Identifier 10.1109/TASE.2006.877393

NOMENCLATURE

GCS (Oxyz)	Global coordinate system.
PCS (O′x′y′z′)	Part coordinate system.
LCS (O″x″y″z″)	Local coordinate system attached to a feature.
HTM	Homogeneous transformation matrix (from A to B means $\mathbf{H}\cdot\mathbf{t}_B=\mathbf{t}_A$).
$\mathbf{q}$, $\mathbf{H}(\mathbf{q})$	Differential motion vector and the associated HTM.
${}^0\mathbf{H}_p$, $\mathbf{H}_p$	HTM from the GCS to the PCS.
$\mathbf{H}(\mathbf{q}_p)$	HTM from the ^{0}PCS to the PCS.
${}^0\mathbf{H}_i$	HTM from the GCS to the ^{0}LCS expressed in ^{0}PCS.
${}^0\mathbf{H}'_i$	HTM from the ^{0}PCS (PCS) to the ^{0}LCS expressed in ^{0}PCS (PCS).
$\mathbf{H}_i$, $(\mathbf{H}'_i)$	HTM from the GCS (PCS) to the LCS.
$\mathbf{H}(\mathbf{q}_i)$, $\mathbf{H}(\mathbf{q}'_i)$	HTM from ^{0}LCS expressed in ^{0}PCS (PCS) to LCS.
$\mathbf{q}_p(\mathbf{q}_p(k))$	Overall deviation of the PCS from its nominal position (at stage k).
$\mathbf{q}'_j$	Overall deviation of the jth feature.
$\mathbf{q}'_{i_k}$	Overall deviation of the feature contacting the kth locator.
$\mathbf{q}'(\mathbf{q}'(k))$	Collective vector regrouping the deviations of the features used as datum (at stage k).
$\mathbf{t}_i$	Position of the ith locator in the GCS.
$\mathbf{T}$	Collective vector of the position of the m locators in the GCS.
$\mathbf{t}'_{i_k}$	Position of the point contacting the kth locator in the PCS.
$\mathbf{T}'$	Vector of the positions of the points contacting the m locators in the PCS.
$\mathbf{n}'_{i_k}$	Norm to the surface at the feature contacting the kth locator in the PCS.
$\mathbf{N}'$	Collective vector of the norms contacting the m locators in the PCS.
$\delta\mathbf{T}$	Error due to the fixture.
$\mathbf{u}_k$	Fixture error for the kth locator.
$\mathbf{U}(\mathbf{U}_k)$	Collective vector regrouping the m fixture errors (at stage k).
$\delta\mathbf{T}'$ and $\delta\mathbf{N}'$	Error due to the location and orientation of the datum.

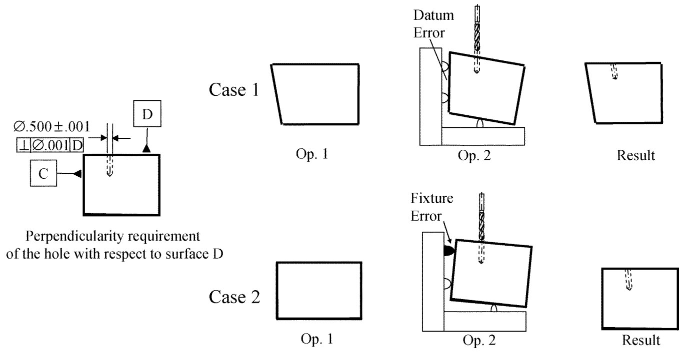

Fig. 1. Illustration of variation propagation.

Φ_i	Contacting condition equation for the ith locator.
$\mathbf{\Phi}$	Collective touching condition equation for the m locators.
J	Jacobian of the constraint equation.
$\mathbf{x}_k(\mathbf{x}_{k+1})$	Stack vector at stage $k(k+1)$ regrouping the deviations of the features.

I. Introduction

MACHINING processes are used to remove materials from a workpiece to obtain higher dimensional accuracy, better surface finishing, or a more complex surface form which cannot be obtained by other processes. Dimensional variation reduction of the product is a crucial engineering objective in both design and manufacturing stages [1], [2]. Unfortunately, variation reduction for machining processes is a challenging problem, particularly for a process that includes multiple operation stages.

A "multistage" machining process refers to a part that is machined through different setups. A multistage machining process might not necessarily contain multiple machining stations. If there are different setups on only one machining station, this machining process is still considered as a multistage machining process. When a workpiece passes through a particular stage of a multistage machining process, the errors of this stage will be accumulated on the workpiece. These errors, in turn, will affect the machining accuracy at subsequent stages. Clearly, for a multistage machining process, product dimensional variation at a certain stage consists of two components: 1) local variation caused by variation sources at current machine stage; and 2) propagated variation due to the machining errors at previous stages. The propagated variation exists because we have to use part features produced at previous stages as the machining datum in the current operation. In multistage assembly processes, the propagated variation is also called reorientation error [3]. This can be illustrated by a simple two-step machining process as shown in Fig. 1. The workpiece is represented as a metal cube (the front view is shown in Fig. 1). Perpendicularity between the drilled hole and surface D represents the workpiece quality and is defined by geometric tolerancing as shown in Fig. 1. In Case 1, the quality problem of Op. 2 is caused by datum error, which is produced at Op. 1. Therefore, the quality variation in case 1 is a propagated variation. In Case 2, the quality problem (nonperpendicularity) is due to a local fixture error. Therefore, the quality variation in case 2 is a local variation at Op. 2. From this example, it is clear that the product dimension quality is a function of local and propagated variation sources in a multistage process.

Owing to the complexity of a machining operation, various types of local error sources exist in a single operation. The error modeling and compensation of local variation is an established field. A substantial body of literature can be found on the modeling and compensation of machine geometric errors [4]–[8]; thermal errors [9]–[12]; fixture-induced errors [13]–[16]; and force-induced errors [17]–[19]. These techniques address the links between product dimensional quality and local process error sources in a single operation.

The propagated variation is caused by the datum feature error produced from previous stations. Due to the complicated interactions among different stages, limited attempts have been made on the variation propagation analysis for a multistage machining process. Lawless *et al.* [20] and Agrawal *et al.* [21] investigated variation transmission in both assembly and machining processes by using a first-order autoregressive model. Jin [22] and Ding *et al.* [23], [24] proposed a state space model to depict variation propagation in a multistage assembly process. However, their approach cannot be applied directly to machining processes. Huang *et al.* [25] proposed a variation propagation model for a multistage machining process. Zhong *et al.* [26] proposed a model to study the variation propagation including workpiece deformation. Still, these are nonlinear or numerical simulation-based models which provide limited physical insights. Most recently, some researchers proposed the use of a state-space model to describe dimensional variation propagation in a multistage machining process [27], [28]. The state-space model provides a good framework for modeling variation propagation. However, the existing techniques require specific fixture setups (e.g., an orthogonal 3-2-1 fixturing layout [29]) and cannot be applied to a general nonorthogonal fixture layout.

In this paper, we develop a state-space modeling technique for dimensional variation propagation of multistage machining processes with general fixture setup schemes. This model allows for a general fixturing scheme beyond the 3-2-1 layouts as well as for non-fully constrained setups. The process and production information are quantitatively integrated into the system matrices of this model. This model can be used for process evaluation and analysis in design and root cause identification in manufacturing for multistage machining processes. The model derivation is presented in Section II. Section III presents a case study to illustrate the derivation and validate the results. Finally, the conclusions and some discussion of the applications of this model are given in Section IV.

II. Derivation of the Variation Propagation Model

A. Problem Formulation

We first identify the boundary of the developed model. There are different ways to classify the process errors. In this paper, we classify the process errors based on their physical sources. Fig. 2 lists the basic process error sources and the dimensional quality evaluation criteria used in engineering practice for a machining

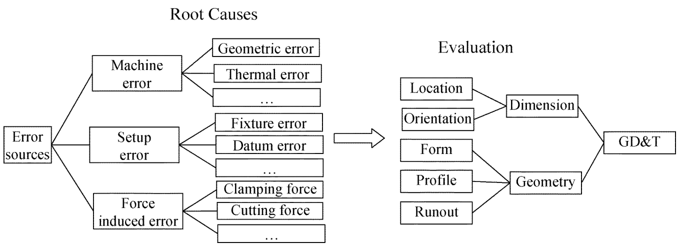

Fig. 2. Machining error sources and evaluation criteria.

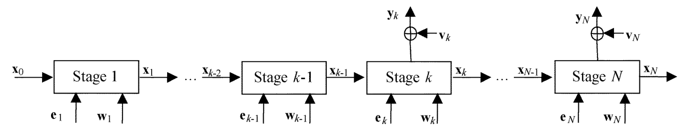

Fig. 3. Diagram of a complicated multistage manufacturing process.

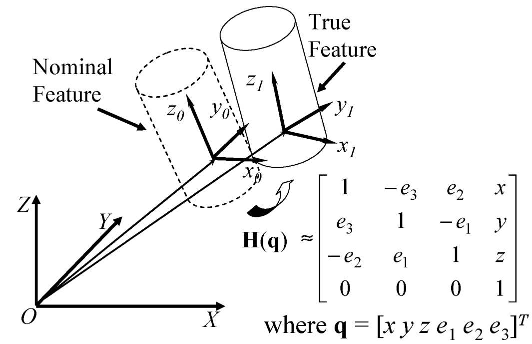

Fig. 4. Concept of the state vector.

process. The process error sources consist of machine errors caused by machine geometric accuracy, thermal error, etc.; setup error due to the fixture and datum errors; and finally, force-induced error caused in part by deformation during cutting. The variation propagation is caused by the datum error. Standards for geometric dimensioning and tolerancing (GD&T) were developed in order to regulate the deviation of the workpiece features. These standards provide a description of the dimensional and geometric accuracy of a workpiece.

Another way of classification is to classify the errors into two categories: systematic and random errors. Systematic errors are constant and repeatable and can be viewed as a constant offset, whereas random errors arise from random fluctuations in the system. This classification overlaps the previous one. For example, the fixture error can be both systematic error (e.g., an error in fixture setup can make one locator consistently higher than the others) and random error (e.g., a locator could become loose and the error direction changes). In the proposed model, we can consider both systematic and random fixture error.

Given the complexity of machining processes, it is very difficult, if not impossible, to develop comprehensive analytical models of the relationship between all error sources and all quality measurements. To limit the scope of this model, in this paper, we focus on the analytical modeling of the relationship between setup errors and dimensional (location and orientation) variation propagation in a multistage process. Since the setup error (datum error in particular) is the key cause of variation propagation, the influence of setup error on product quality will be thoroughly studied through kinematic analysis. Although other types of errors are not studied in this paper, interfaces to other errors are included in the developed model, making the model flexible: the model can be extended to include other errors components influencing the product quality (e.g., thermal error). The rationality for considering only dimensional instead of both dimensional and geometric variations is that this model focuses on describing the machining variation propagation among different stages. Since most of the geometric variation is determined on a single stage and remains unchanged throughout the whole process, it is unnecessary to build a model describing its propagation. Therefore, geometric variation is not included in this model.

In order to model variation propagation in complex multistage manufacturing processes, a chain-like state transition framework as used in [28] is adopted here (Fig. 3).

For a N-stage process, the model is in the form of

$$\mathbf{x}_k = \mathbf{A}_{k-1}\mathbf{x}_{k-1} + \mathbf{B}_k\mathbf{e}_k + \mathbf{w}_k \text{ and } \mathbf{y}_k = \mathbf{C}_k\mathbf{x}_k + \mathbf{v}_k \quad (1)$$

where $k = 1, 2, \ldots, N$ is the stage index. The key quality characteristics of the product (e.g., dimensional deviations of key features) after each stage are represented by the state vector $\mathbf{x}_k$. The state vector $\mathbf{x}_k$ is a stack of random variables. The datum errors are incorporated in $\mathbf{x}_k$ and, thus, the propagated variation is captured by $\mathbf{A}_{k-1}\mathbf{x}_{k-1}$. The local process errors (e.g., fixturing errors and machine errors) are denoted by $\mathbf{e}_k$. Therefore, the local variation is captured by $\mathbf{B}_k\mathbf{e}_k$. The vector $\mathbf{e}_k$ is a random vector that accounts for both systematic and random local errors. For example, a mean shift of a variable in $\mathbf{e}_k$ can describe a systematic error of a locating pin consistently higher than the others; and the variance of a variable in $\mathbf{e}_k$ can describe a random error of a loose locating pin moving in different directions.

For our purpose, we will focus on the derivation of $\mathbf{A}_k$ and $\mathbf{B}_k$ corresponding to the datum and fixture errors. However, it is clear that this model is flexible enough to incorporate errors from other processes given the open structure of the model as shown in (1). Natural variation and unmodeled errors in the process are represented by a noise input to the system $\mathbf{w}_k$. The product quality measurements are collected in $\mathbf{y}_k$. The measurement noise, including systematic and random measurement errors, is denoted by vector $\mathbf{v}_k$.

In this paper, in order to capture the dimensional quality, including the position and orientation of the key features of the product, the state vector $\mathbf{x}_k$ is defined as a stack of differential motion vectors [31], [32] that represent the position and orientation deviations of the key features. This concept is illustrated in Fig. 4 utilizing a cylindrical feature. The design nominal location and orientation of the cylindrical feature can be represented by a local coordinate system $x_0y_0z_0$. The true location and orientation of the cylinder after machining can be represented by another local coordinate system $x_1y_1z_1$. Then, the dimensional error of this feature can be represented by a homogeneous transformation matrix (HTM) from $x_0y_0z_0$ to $x_1y_1z_1$. For small errors, the HTM from $x_0y_0z_0$ to $x_1y_1z_1$ can be approximated in the format shown in Fig. 4. The translational deviation, denoted as $[x, y, z]^{\mathrm{T}}$, and the orientation deviation, denoted

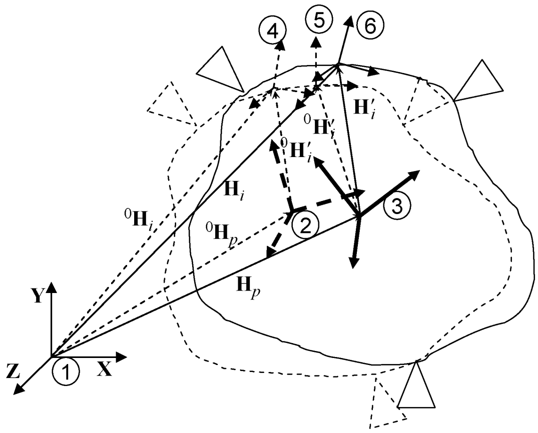

Fig. 5. Errors and their accumulation in a machining operation.

as $[e_1, e_2, e_3]^{\mathrm{T}}$, can be stacked up to form a differential motion vector [31], [32]. Using this 6 by 1 vector, the deviation of both the location and the orientation can be captured. This representation is also consistent with the working principle of the modern computer-aided design/computer-aided manufacturing (CAD/CAM) system and the coordinate measurement machine (CMM) [33], [34], a popularly used dimensional quality inspection device. We can easily evaluate the deviations of features in terms of the vector by comparing the nominal design with the CMM output.

The complicated variation propagation is handled automatically in this model through the state transitions. To construct this model, we need to study locally the relationship among $\mathbf{x}_{k-1}$, $\mathbf{x}_k$, and $\mathbf{e}_k$ at each individual stage k. In the following section, we will systematically investigate this relationship to provide an analytical expression of the coefficient matrices for a general multistage machining process.

B. Model Derivation

A machining operation at a particular stage includes three steps: 1) locating and clamping the part in a fixture; 2) placing the fixture on the machine working table (for some dedicated machines, the fixture is already built in the machine); and 3) cutting the part to desired specifications. To describe the dimensional errors involved in the whole operation, six coordinate systems are involved as illustrated by Fig. 5. The dash-line object in Fig. 5 represents the nominal location of the workpiece and the solid-line object indicates the true location.

These coordinate systems are described as follows:

1) Coordinate system (CS) 1 is the global coordinate system that is often selected as the machine coordinate system.
2) CS 2 is the design nominal part coordinate system which represents where the part should be located under ideal conditions.
3) CS 3 is the actual part coordinate system. The deviation between CS 2 and CS 3 is due to fixture and datum errors. This deviation can be represented by a differential motion vector $\mathbf{q}_p$.
4) CS 4 is the nominal coordinate system of the ith feature of the part with respect to CS 2. As new features are generated through cutting, CS 4 is also the nominal coordinate system locating the ith cutting tool path.
5) CS 5 is the nominal coordinate system of the ith feature of the part with respect to CS 3. Please note that the transformation from CS 2 to CS 4 and the transformation from CS 3 to CS 5 is the same.
6) CS 6 represents the true location of the ith feature. It is also the true location of the ith cutting tool path.

The transformations between these coordinate systems are also labeled in the figure. In addition to those transformations, $\mathbf{H}(\mathbf{q}_p)$, $\mathbf{H}(\mathbf{q}_i)$, and $\mathbf{H}(\mathbf{q}'_i)$ are the homogeneous transformation from CS 2 to CS 3, from CS 4 to CS 6, and from CS 5 to CS 6, respectively, where $\mathbf{H}(\mathbf{q})$ is defined as the homogeneous transformation matrix determined by a differential motion vector $\mathbf{q}$ as shown in Fig. 4. The following notation is used in this paper. The left superscript 0 indicates the nominal values. A notation without prime indicates a value with respect to the global coordinate system. A notation with prime indicates a value with respect to the part coordinate system. A notation with double prime indicates a value with respect to the local feature coordinate system. Please refer to the nomenclature section for a comprehensive list of notations.

From the aforementioned description, it is clear that the ideal location of the newly generated ith feature should be at CS 5, corresponding to the position of the nominal feature in the true part coordinate system. However, since the final location of the newly generated feature is at CS 6, where the cutting tool is, we need to find the value of $\mathbf{q}'_i$ that represents the deviation between CS 5 and CS 6. This deviation can be decomposed into two sources: 1) the deviation from CS 4 to CS 6, which is due to the geometric error of the machine and 2) the deviation from CS 4 to CS 5, caused by datum and fixturing errors. The machining errors $\mathbf{q}_i$ can be further decomposed into thermal, geometric, and/or cutting force-induced errors. In order to determine the deviation from CS 4 to CS 5, we developed a general analysis procedure to obtain the model linking the fixture error, datum error, and the deviation of the part coordinate system, represented by $\mathbf{q}_p$. The fixture error is denoted as $\mathbf{u}_k$ for the kth locator, which is a 3 by 1 vector representing the deviation of the locator from its nominal position. The datum error is the deviation of the datum feature produced in previous stages and, thus, it is denoted as $\mathbf{q}'_j$, where j is the feature index of the datum features at the current stage. Upon obtaining $\mathbf{q}_p$, the deviation from CS 4 to CS 6 can also be obtained. The final feature deviation can be achieved by combining the impacts of fixture errors, datum errors, and machine errors together.

The following steps are involved in the derivation of $\mathbf{q}'_i$.

Step 1) Derivation of $\mathbf{q}_p$ given fixture and datum errors.

A simple fixturing scheme with one locator is shown in Fig. 6. Oxyz represent the global coordinate system (GCS); O$'$x$'$y$'$z$'$ represent the part coordinate system (PCS). If the ith locator is in contact with the part surface at the ith contact point, then the tangent plane to the surface at the ith point is

$$\mathbf{n}'^{T}_i \cdot \mathbf{t}' - \mathbf{n}'^{T}_i \cdot \mathbf{t}'_i = 0 \tag{2}$$

where $\mathbf{t}'_i$ represents the location in the PCS of the ith contact point of the ith locator on the part and $\mathbf{n}'_i$ is the outgoing normal vector of the part surface at that ith contact point. As the ith locator has to be on

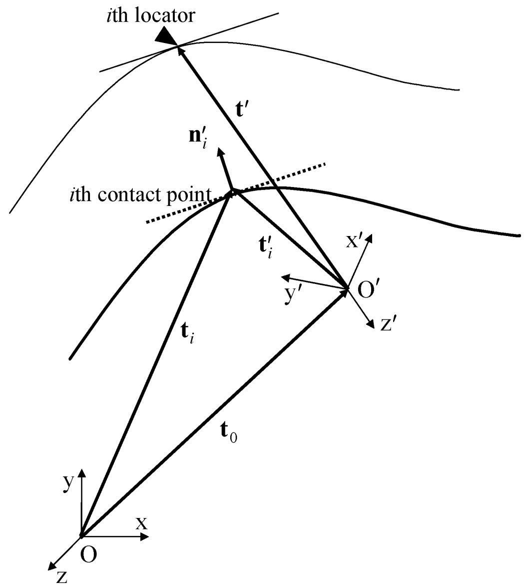

Fig. 6. Contact condition for a 3-D workpiece.

the tangent surface which satisfies (2), we have the constraint equation of the contact condition for the ith locator [35]

$$\Phi_i = \mathbf{n}_i'^T \cdot \mathbf{R}_p^T \cdot (\mathbf{t}_i - \mathbf{t}_p) - \mathbf{n}_i'^T \cdot \mathbf{t}_i' = 0 \tag{3}$$

where $\mathbf{R}_p$ is the rotational matrix and $\mathbf{t}_p$ is the translational component of the homogeneous transformation matrix $\mathbf{H}_p = \begin{bmatrix} \mathbf{R}_p & \mathbf{t}_p \\ \mathbf{0} & 1 \end{bmatrix}$ from the PCS to the GCS and $\mathbf{t}_i$ is the coordinate of the ith locator in the GCS. The expression $\mathbf{R}_p^T \cdot (\mathbf{t}_i - \mathbf{t}_p)$ actually transforms $\mathbf{t}_i$ into the PCS. The physical interpretation of (3) is that the locator and the contact point on the part should be in the same tangent plane.

For a fixturing scheme with m locators, the m constraint equations for contact conditions can be combined together to obtain an equation system

$$\mathbf{\Phi} = [\Phi_1, \ldots, \Phi_m]^T = \mathbf{0}. \tag{4}$$

By defining $\mathbf{T} \equiv [\mathbf{t}_1^T \cdots \mathbf{t}_m^T]^T$, $\mathbf{T}' \equiv [\mathbf{t}_{i_1}'^T \ldots \mathbf{t}_{i_m}'^T]^T$, $\mathbf{N}' \equiv \begin{bmatrix} \mathbf{n}_{i_1}'^T & & 0 \\ & \ddots & \\ 0 & & \mathbf{n}_{i_m}'^T \end{bmatrix}$ where i_k represents the index of the feature contacting the kth locator, $\mathbf{d}_p \equiv [\mathbf{t}_p^T\, \boldsymbol{\omega}_p^T]^T$ and $\boldsymbol{\omega}_p$ contain the three Euler angles of the rotational matrix $\mathbf{R}_p$ and (4) can be expressed as

$$\mathbf{\Phi}(\mathbf{d}_p, \mathbf{T}, \mathbf{T}', \mathbf{N}') = \mathbf{0}. \tag{5}$$

Clearly, errors in datum (a deviation in $\mathbf{T}'$ and $\mathbf{N}'$) and fixture (a deviation in $\mathbf{T}$) will cause deviations in $\mathbf{d}_p$ in order to make (5) valid. If the errors are infinitesimal, the relationship among $\delta\mathbf{d}_p$ (denoted

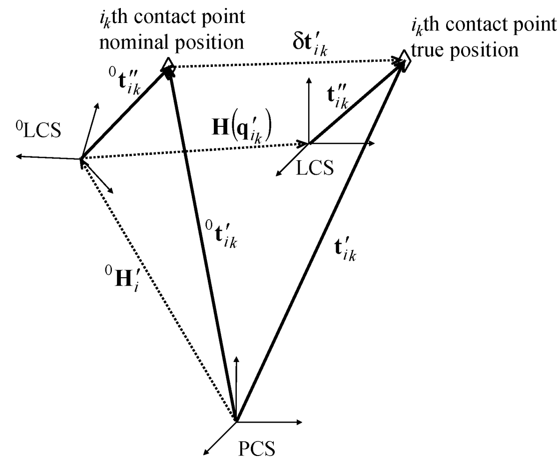

Fig. 7. Deviation of the i_kth contact point.

as $\mathbf{q}_p$), $\delta\mathbf{T}$, $\delta\mathbf{T}'$, and $\delta\mathbf{N}'$ can be obtained through a differentiation operation in (5) as

$$\frac{\partial \mathbf{\Phi}}{\partial \mathbf{d}_p}\delta\mathbf{d}_p = -\left[\frac{\partial \mathbf{\Phi}}{\partial \mathbf{T}}\delta\mathbf{T} + \frac{\partial \mathbf{\Phi}}{\partial \mathbf{T}'}\delta\mathbf{T}' + \frac{\partial \mathbf{\Phi}}{\partial \mathbf{N}'}\delta\mathbf{N}'\right]. \tag{6}$$

Clearly, from (3), the term $\partial\mathbf{\Phi}/\partial\mathbf{N}'$ is always equal to zero; the right-hand side of (6) has, therefore, only two non-zero terms. The term $\delta\mathbf{T}$ captures the variation due to the fixture error. The term $\delta\mathbf{T}'$ captures the contribution of the datum error which corresponds to the contribution of both the location and orientation deviations of the datum.

Equation (6) has to be rearranged to (7), where $\mathbf{U} = [\mathbf{u}_1^T \cdots \mathbf{u}_m^T]^T = \delta\mathbf{T}$, corresponding to the fixture error for the m locators and $\mathbf{q}' = [\mathbf{q}_{i_1}'^T \ldots \mathbf{q}_{i_k}'^T \ldots \mathbf{q}_{i_m}'^T]^T$ containing the datum errors produced in previous stages

$$\frac{\partial \mathbf{\Phi}}{\partial \mathbf{d}_p}\mathbf{q}_p = \mathbf{F}_1 \cdot \mathbf{U} + \mathbf{F}_2 \cdot \mathbf{q}'. \tag{7}$$

The expressions of $\mathbf{F}_1$ and $\mathbf{F}_2$ can be calculated from the nominal values of the parameters.

Step 2) Calculation of $\mathbf{F}_1$.

Substituting $\mathbf{u}$ to $\delta\mathbf{T}$, $\mathbf{F}_1$ is directly obtained as

$$\mathbf{F}_1 = -\frac{\partial \mathbf{\Phi}}{\partial \mathbf{T}} = -\mathbf{N}' \cdot \begin{bmatrix} \mathbf{R}_p^T & & \\ & \ddots & \\ & & \mathbf{R}_p^T \end{bmatrix}.$$

Step 3) Calculation of $\mathbf{F}_2$.

The derivation procedure of $\mathbf{F}_2$ is illustrated in Fig. 7. The vector $\delta\mathbf{T}' \equiv [\delta\mathbf{t}_{i_1}'^T \ldots \delta\mathbf{t}_{i_m}'^T]^T$ corresponds to the collective vector of the deviations of the datum. $\delta\mathbf{t}_{i_k}'$ contains information about the location error of the contact point on the feature touching the kth locator. As shown in Fig. 7, this error can be expressed as $\delta\mathbf{t}_{i_k}' = \mathbf{t}_{i_k}' - {}^0\mathbf{t}_{i_k}'$. In other words, this error is expressed as the difference in the PCS of the true and the nominal position of the contact point. ${}^0\mathbf{t}_{i_k}'$ is known from the nominal conditions, because the contact point has the same position as the nominal position of the kth locator under nominal conditions. The value of $\mathbf{t}'_{i_k}$ can be determined using homogeneous transformation matrices from PCS to LCS as

$$\begin{bmatrix}\mathbf{t}'_{i_k}\\1\end{bmatrix} = \left({}^0\mathbf{H}'_i\right)\cdot\mathbf{H}\left(\mathbf{q}'_{i_k}\right)\cdot\begin{bmatrix}\mathbf{t}''_{i_k}\\1\end{bmatrix} \tag{8}$$

where $\mathbf{t}''_{i_k}$ is the location of the kth contact point expressed in the true local feature coordinate system. From the small deviation assumption, we assume that the contact location expressed in the feature local coordinate system is unchanged (i.e., $\mathbf{t}''_{i_k} = {}^0\mathbf{t}''_{i_k}$). Therefore, by substituting $\left[\begin{smallmatrix}\mathbf{t}''_{i_k}\\1\end{smallmatrix}\right] = \left[\begin{smallmatrix}{}^0\mathbf{t}''_{i_k}\\1\end{smallmatrix}\right] = \left({}^0\mathbf{H}'_i\right)^{-1}\cdot\left[\begin{smallmatrix}{}^0\mathbf{t}'_{i_k}\\1\end{smallmatrix}\right]$ into (8), we have

$$\begin{bmatrix}\mathbf{t}'_{i_k}\\1\end{bmatrix} = \left({}^0\mathbf{H}'_i\right)\cdot\mathbf{H}\left(\mathbf{q}'_{i_k}\right)\cdot\left({}^0\mathbf{H}'_i\right)^{-1}\cdot\begin{bmatrix}{}^0\mathbf{t}'_{i_k}\\1\end{bmatrix}. \tag{9}$$

Based on (9), finally, we can obtain $\delta\mathbf{t}'_{i_k}$ as

$$\begin{bmatrix}\delta\mathbf{t}'_{i_k}\\0\end{bmatrix} = \left({}^0\mathbf{H}'_i\right)\cdot\left[\mathbf{H}\left(\mathbf{q}'_{i_k}\right)-\mathbf{I_4}\right]\cdot\left({}^0\mathbf{H}'_i\right)^{-1}\cdot\begin{bmatrix}{}^0\mathbf{t}'_{i_k}\\1\end{bmatrix}. \tag{10}$$

Equation (10) links the deviation of the coordinate system attached to the feature in contact with the kth locator with the deviation of the contact point in the PCS. By assembling together the values $\delta\mathbf{t}'_{i_k}$, $\delta\mathbf{T}'$ can be obtained. Noticing that $\partial\mathbf{\Phi}/\partial\mathbf{T}' = -\mathbf{N}'$ from the variation equation (6), the linear equation system $\mathbf{N}'\cdot\delta\mathbf{T}' = \mathbf{F}_2\cdot\mathbf{q}'$ can be solved to obtain the matrix $\mathbf{F}_2$. The general expression of $\mathbf{F}_2$ is listed in the Appendix.

Step 4) Calculation of the Jacobian ($\partial\mathbf{\Phi}/\partial\mathbf{d}_p$).

The term $\partial\mathbf{\Phi}/\partial\mathbf{d}_p$ is the Jacobian $\mathbf{J}$ of the collective contact condition (4). The calculation of the Jacobian is discussed in the following.

The Jacobian $\mathbf{J}$ of the collective contact condition (4) can be expressed as $\mathbf{J} = [\mathbf{J}_1^T \cdots \mathbf{J}_m^T]^T$, where $\mathbf{J}_k$ is a 1 by 6 vector as shown in the equation at the bottom of the page, where $\mathbf{d}_p \equiv [\mathbf{t}_p^T\ \boldsymbol{\omega}_p^T]^T = [x_p, y_p, z_p, e_1, e_2, e_3]^T$ denotes the parameters of the six degrees of freedom of the part. Without loss of generality, we can take the GCS as the same as the nominal PCS. In that case, $\mathbf{R}_p$ is the identity matrix and a small deviation of the part can be represented by a homogeneous transformation matrix $\mathbf{H}_p$ with $\mathbf{R}_p = \begin{bmatrix}1 & -e_3 & e_2\\ e_3 & 1 & -e_1\\ -e_2 & e_1 & 1\end{bmatrix}$; then, we can explicitly calculate $\mathbf{J}_k$ as

$$\begin{aligned}\mathbf{J}_k = \big[&-n'_{i_kx}\ \ -n'_{i_ky}\ \ -n'_{i_kz}\ \ \left(n'_{i_ky}\cdot{}^0t'_{i_kz} - n'_{i_kz}\cdot{}^0t'_{i_ky}\right)\\ &\left(n'_{i_kz}\cdot{}^0t'_{i_kx} - n'_{ix}\cdot{}^0t'_{i_kz}\right)\ \ \left(n'_{i_kx}\cdot{}^0t'_{i_ky} - n'_{i_ky}\cdot{}^0t'_{i_kx}\right)\big]\end{aligned}$$

where n'_{i_kx}, n'_{i_ky}, and n'_{i_kz} are the three components in the PCS of the outgoing norm to the surface contacting the kth locator and t'_{i_kx}, t'_{i_ky}, and t'_{i_kz} are the three components of $\mathbf{t}'_{i_k}$, respectively. All of the parameters involved in the calculation of the Jacobian are known from the nominal condition.

The Jacobian is nonsingular if the workpiece is deterministically located; in that case, the part is fully constrained in its 6 degrees of freedom and (11) links the overall resulting error $\mathbf{q}_p$ with the composition of datum and fixture errors

$$\mathbf{q}_p = \mathbf{J}^{-1}\cdot(\mathbf{F}_1\cdot\mathbf{U} + \mathbf{F}_2\cdot\mathbf{q}'). \tag{11}$$

The part is said to be not fully constrained if it has at least one degree of freedom after being mounted in the fixture. In that case, the Jacobian is singular and the overall error cannot be directly calculated. If the part has n degrees of freedom, n artificial locators need to be added to the existing locators in order to fully constrain the part. The Jacobian becomes nonsingular and the model can be derived. The numerical result for the deviations in the directions constraint by the artificial locators does not have any physical meaning. Therefore, those deviations are set to a constant value, for example zero, as if there was no deviation in those directions. However, since the locators controlling those directions are artificial, the feature deviations in those directions cannot be used as known datum deviations in the following stations.

C. Derivation of $\mathbf{q}'_i$ of the ith Newly Generated Feature

Given the deviation $\mathbf{q}_p$ of the PCS with respect to the GCS due to the datum and fixture error and the deviation of the cutting tool regarding the GCS due to the machine geometry error $\mathbf{q}_i$, the final deviation $\mathbf{q}'_i$ of the newly generated feature in PCS can be obtained based on the following identity:

$$\mathbf{H}\left(\mathbf{q}'_i\right) = \left({}^0\mathbf{H}'_i\right)^{-1}\cdot\mathbf{H}(\mathbf{q}_p)^{-1}\cdot\left({}^0\mathbf{H}'_i\right)\cdot\mathbf{H}(\mathbf{q}_i). \tag{12}$$

$$\begin{aligned}\mathbf{J}_k = \Bigg[&\left(-\mathbf{n}'^{\,T}_{i_k}\cdot\mathbf{R}_p^T\cdot\frac{\partial\mathbf{t}_p}{\partial x_p}\right)\left(-\mathbf{n}'^{\,T}_{i_k}\cdot\mathbf{R}_p^T\cdot\frac{\partial\mathbf{t}_p}{\partial y_p}\right)\left(-\mathbf{n}'^{\,T}_{i_k}\cdot\mathbf{R}_p^T\cdot\frac{\partial\mathbf{t}_p}{\partial z_p}\right)\cdots\\ &\cdots\left(\mathbf{n}'^{\,T}_{i_k}\cdot\frac{\partial\mathbf{R}_p^T}{\partial e_1}\cdot\mathbf{t}'_{i_k}\right)\left(\mathbf{n}'^{\,T}_{i_k}\cdot\frac{\partial\mathbf{R}_p^T}{\partial e_2}\cdot\mathbf{t}'_{i_k}\right)\left(\mathbf{n}'^{\,T}_{i_k}\cdot\frac{\partial\mathbf{R}_p^T}{\partial e_3}\cdot\mathbf{t}'_{i_k}\right)\Bigg]\end{aligned}$$

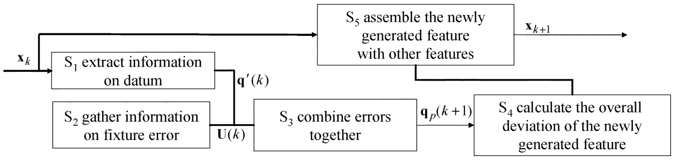

Fig. 8. Steps of the derivation of variation propagation model.

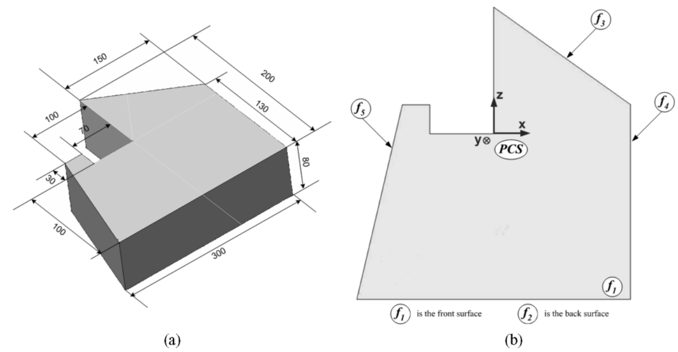

Fig. 9. Workpiece for the case study. (a) Isometric view. (b) Top view.

The details of the derivation are as follows:

Considering Fig. 5, the homogeneous transformation from CS 2 to CS 6 can be obtained in two ways: 1) from CS 2 to CS 4 and then to CS 6; 2) from CS 2 to CS 3 to CS 5 and then to CS 6. In the former, the homogeneous transformation matrix from CS2 to CS 6 can be obtained as $({}^0\mathbf{H}_i') \cdot \mathbf{H}(\mathbf{q}_i)$. In the latter, the same homogeneous transformation matrix can be obtained as $\mathbf{H}(\mathbf{q}_p) \cdot ({}^0\mathbf{H}_i') \cdot \mathbf{H}(\mathbf{q}_i')$.

Hence, we have $({}^0\mathbf{H}_i') \cdot \mathbf{H}(\mathbf{q}_i) = \mathbf{H}(\mathbf{q}_p) \cdot ({}^0\mathbf{H}_i') \cdot \mathbf{H}(\mathbf{q}_i')$ and, thus, (12) can be obtained.

In (12), $\mathbf{q}_p$ and $\mathbf{q}_i$ are small values and, thus, the multiplication terms among the components of these terms can be neglected. By ignoring these multiplication terms, the relationship among $\mathbf{q}_i'$, $\mathbf{q}_p$, and $\mathbf{q}_i$ are still linear. Without loss of generality, we have

$$\mathbf{q}_i' = \mathbf{F}_3 \cdot \mathbf{q}_p + \mathbf{F}_4 \cdot \mathbf{q}_i. \tag{13}$$

The derivation of $\mathbf{F}_3$ and $\mathbf{F}_4$ is straightforward from (12) although the expression is tedious. The details are omitted here.

Combining (11) and (13), the deviation of the ith newly generated feature can be obtained as

$$\mathbf{q}_i' = \mathbf{F}_3 \cdot \mathbf{J}^{-1} \cdot \mathbf{F}_2 \cdot \mathbf{q}' + \mathbf{F}_3 \cdot \mathbf{J}^{-1} \cdot \mathbf{F}_1 \cdot \mathbf{U} + \mathbf{F}_4 \cdot \mathbf{q}_i. \tag{14}$$

The first term on the right-hand side of (14) represents the propagated errors from the previous operations because $\mathbf{q}'$ is a collection of the deviations of datum features that are produced in previous operations. The second term represents the fixture error at the current stage and the third term represents machine geometric errors. By assembling the deviations of all newly generated features and linking different stages together, a comprehensive variation propagation model in state transition form can be obtained. The details of this final step of the model derivation are presented in the following section.

D. Linking Multistage Together

Fig. 8 shows the steps of the variation propagation model. The letter k corresponds to the stage index. The vector of $\mathbf{x}_k$ is a collection of quality deviations of all key features on the product after the kth stage. The deviation of each feature is represented by a 6 by 1 differential vector as illustrated in Fig. 4. If a feature has not been generated after the kth stage, the corresponding components of that feature in $\mathbf{x}_k$ are set to be zero, and after it has been generated, the zero components are replaced by nonzero deviations. The detailed procedure explaining each step is presented below.

S1) Only the dimensional quality of the datum features will have an influence on the deviation of the newly generated feature; therefore, we collect from $\mathbf{x}_k$ the dimensional deviation of the datum features after the kth stage to create the vector $\mathbf{q}'(k)$, where $\mathbf{q}'(k)$ contains the deviations of all the datum features at the $(k+1)$th stage. We use k as the index in $\mathbf{q}'(k)$ since these features are produced up to the kth stage.

S2) Gather the in-process information on fixture nominal position and fixture error $\mathbf{U}(k)$.

S3) From the $\mathbf{q}'(k)$ and the fixture error $\mathbf{U}(k)$, find $\mathbf{q}_p(k+1)$ as in (11).

S4) Calculate the dimensional error for all newly generated features $\mathbf{q}_i'$, i is from 1 to the total number of new features, using (14) and the associated procedures.

S5) Assemble the deviations of the newly generated features and $\mathbf{x}_k$ together (i.e., replace the components corresponding to each ith newly generated features in $\mathbf{x}_k$ by their deviation $\mathbf{q}_i'$ to obtain vector $\mathbf{x}_{k+1}$).

This procedure can be repeated for each stage and, finally, a chain-like state transition model can be achieved. In the next section, a practical case study is presented to illustrate the effectiveness of this modeling technique.

III. Validation of the State-Space Variation Propagation Model

The developed variation propagation modeling technique is validated on a multistage machining process. In this section, we first introduce the process; then, the variation propagation model is developed and, finally, results are validated.

A. Introduction to the Multistage Machining Process

The presented machining process is adapted from a real machining process with modifications due to confidentiality considerations. It has two stages and one feature will be machined on the workpiece at each stage through end milling.

The first operation step is to mill the top face f_1. The datums of this operation are the feature f_2, feature f_3, and feature f_4. Clearly, this fixture layout is not a traditional 3-2-1 layout since the datums are not orthogonal to each other. The second operation consists of machining the inclined side f_5 of the workpiece. The datums for this operation are feature f_3, feature f_1, and feature f_4. All features are labeled in Fig. 9.

Coordinate systems are defined on each feature. The nominal position of the features is therefore known with respect to the

TABLE I
NOMINAL POSITIONS AND ORIENTATIONS OF KEY FEATURES

Feature Name	${}^{0}\boldsymbol{\omega}_i^R$	${}^{0}\mathbf{t}_i^R$
f_1	[π/2, 0, 0]	[-30, 0, 0]
f_2	[-π/2, 0, 0]	[0, 80, 0]
f_3	[0, 0.588, 0]	[0, 0, 100]
f_4	[0, π/2, 0]	[150, 40, -85]
f_5	[0, -π-0.86, 0]	[-100, 0, 30]

TABLE II
NOMINAL POSITION OF THE LOCATORS IN THE GCS

Op#	Locator index k	From feature	$\mathbf{t}_k = {}^{0}\mathbf{t}'_{i_k}$	$\mathbf{n}'_{i_k}$	Fixture error
1	1	f_2	$[-100\ 80\ -100]^T$	$[0\ 1\ 0]^T$	$[0\ 0.1\ 0]^T$
	2	f_2	$[20\ 80\ 80]^T$	$[0\ 1\ 0]^T$	$[0\ 0.1\ 0]^T$
	3	f_2	$[100\ 80\ 0]^T$	$[0\ 1\ 0]^T$	$[0\ -0.05\ 0]^T$
	4	f_3	$[45\ 40\ 100]^T$	$[0.5547\ 0\ 0.8320]^T$	$[0\ 0\ -0.1]^T$
	5	f_3	$[75\ 40\ 80]^T$	$[0.5547\ 0\ 0.8320]^T$	$[0.05\ 0\ 0.1]^T$
	6	f_4	$[150\ 40\ -85]^T$	$[0\ 0\ 1]^T$	$[0.1\ 0\ 0]^T$
2	1	f_3	$[45\ 20\ 100]^T$	$[0.5547\ 0\ 0.8320]^T$	$[0.1\ 0\ 0]^T$
	2	f_3	$[75\ 60\ 80]^T$	$[0.5547\ 0\ 0.8320]^T$	$[0.1\ 0\ 0]^T$
	3	f_3	$[120\ 20\ 50]^T$	$[0.5547\ 0\ 0.8320]^T$	$[0.1\ 0\ 0]^T$
	4	f_1	$[-100\ 0\ 100]^T$	$[0\ -1\ 0]^T$	$[0\ -0.3\ 0]^T$
	5	f_1	$[100\ 0\ 0]^T$	$[0\ -1\ 0]^T$	$[0\ -0.3\ 0]^T$
	6	f_4	$[150\ 40\ -85]^T$	$[1\ 0\ 0]^T$	$[0.05\ 0\ 0]^T$

PCS by a homogeneous transformation matrix. Table I gathers the HTM components for each feature.

The nominal location and orientation of the locators, expressed in PCS (in this case, we take GCS the same as PCS for sake of simplicity), are given in Table II. Table II also lists the information about the outgoing normal direction of the datum at the nominal contact points. This information is required to develop the variation propagation model. The last column presented in Table II is the systematic fixture error $\mathbf{u}_k$ intentionally added in the model for validation purposes. The nonzero values in $\mathbf{u}_k$ correspond to the magnitudes of the fixture errors. Therefore, the nominal positions in GCS of the locators listed in Table II are also the nominal positions in the PCS of the contact points on the part.

Following the procedure shown in Section II, a variation propagation model can be obtained for this two-stage machining process and measurement values are predicted.

B. Model Derivation for Stage 1

The workpiece in stage 1 is assumed to be nominal; therefore, $\mathbf{x}_1 = \mathbf{0}_{30\times 1}$. By following the procedure developed in Section II-B, we obtain $\mathbf{F}_1$, shown in the first equation at the bottom of the page. Together with

$$\mathbf{U} = [0 \quad 0.1 \quad 0 \quad 0 \quad 0.1 \quad 0 \quad 0 \quad -0.05 \quad 0 \quad 0 \quad 0 \quad -0.1 \quad 0.05 \quad 0 \quad 0.1 \quad 0.1 \quad 0 \quad 0]^T$$

we have the contribution of the fixture error to $\mathbf{q}_p$.

Since the part is considered as nominal, there is no datum error in this stage. Therefore, the expression of $\mathbf{F}_2$ will not be given here since it has no contribution to the overall error.

The Jacobian is calculated from nominal conditions as shown in the second equation at the bottom of the page. By assembling the two sources of error together, we obtain the deviation $\mathbf{q}_p$ of the PCS. This result is listed in Table IV. This vector represents the deviation of the part coordinate system given the datum and fixture errors.

$$\mathbf{F}_1 = \begin{bmatrix} 0 & -1 & 0 & 0 & 0 & 0 & 0 & 0 & 0 & 0 & 0 & 0 & 0 & 0 & 0 & 0 & 0 & 0 \\ 0 & 0 & 0 & 0 & -1 & 0 & 0 & 0 & 0 & 0 & 0 & 0 & 0 & 0 & 0 & 0 & 0 & 0 \\ 0 & 0 & 0 & 0 & 0 & 0 & 0 & -1 & 0 & 0 & 0 & 0 & 0 & 0 & 0 & 0 & 0 & 0 \\ 0 & 0 & 0 & 0 & 0 & 0 & 0 & 0 & 0 & -0.5547 & 0 & -0.83205 & 0 & 0 & 0 & 0 & 0 & 0 \\ 0 & 0 & 0 & 0 & 0 & 0 & 0 & 0 & 0 & 0 & 0 & 0 & -0.5547 & 0 & -0.83205 & 0 & 0 & 0 \\ 0 & 0 & 0 & 0 & 0 & 0 & 0 & 0 & 0 & 0 & 0 & 0 & 0 & 0 & 0 & -1 & 0 & 0 \end{bmatrix}$$

$$\mathbf{J} = \begin{bmatrix} 0 & -1 & 0 & -100 & 0 & 100 \\ 0 & -1 & 0 & 80 & 0 & -20 \\ 0 & -1 & 0 & 0 & 0 & -100 \\ -0.5547 & 0 & -0.83205 & -33.282 & -18.0278 & 22.1880 \\ -0.5547 & 0 & -0.83205 & -33.282 & 18.0278 & 22.1880 \\ -1 & 0 & 0 & 0 & 85 & 40 \end{bmatrix}$$

By following the procedure in Section II-B, we calculate the deviation of the newly created feature, the front face f_1, given its nominal position in the PCS, known by

$$
{}^{0}\mathbf{H}'_{\mathbf{f}_1} = \begin{bmatrix} 1 & 0 & 0 & 30 \\ 0 & 0 & 1 & 0 \\ 0 & -1 & 0 & 0 \\ 0 & 0 & 0 & 0 \end{bmatrix}. \text{ We first obtain } \mathbf{F}_3:
$$

$$
\mathbf{F}_3 = \begin{bmatrix} -1 & 0 & 0 & 0 & 0 & 0 \\ 0 & 0 & 1 & 0 & -30 & 0 \\ 0 & -1 & 0 & 0 & 0 & -30 \\ 0 & 0 & 0 & -1 & 0 & 0 \\ 0 & 0 & 0 & 0 & 0 & 1 \\ 0 & 0 & 0 & 0 & -1 & 0 \end{bmatrix}.
$$

In this case study, it is understood that there is no machine error (i.e., $\mathbf{H}(\mathbf{q}_i) = \mathbf{I}_{4\times4}$). Since the PCS is taken as the GCS, $\mathbf{q}_i$ represents the machine error in the GCS as well as in the PCS. Therefore, $\mathbf{F}_4 = \mathbf{I}_{6\times6}$. We obtain $\mathbf{q}'_{\mathbf{f}_1}$ and we update $\mathbf{x}_1$ to $\mathbf{x}_2 = [\mathbf{q}'^{\,T}_{\mathbf{f}_1}\ \mathbf{0}_{1\times6}\ \mathbf{0}_{1\times6}\ \mathbf{0}_{1\times6}\ \mathbf{0}_{1\times6}]^T$.

C. Model Derivation for Stage 2

The procedure developed in Section II-B is also followed here.

First, the contribution of the fixture error is determined by the location error of the PCS by calculating $\mathbf{F}_1$ shown in the first equation at the bottom of the page with

$$
\mathbf{U} = [0.1\ \ 0\ \ 0\ \ 0.1\ \ 0\ \ 0\ \ 0.1\ \ 0\ \ 0\ \ 0\ \ -0.3\ \ 0\ \ 0\ \ -0.3\ \ 0\ \ 0.05\ \ 0\ \ 0]^T.
$$

Since the secondary datum used in stage 2 is the feature created during stage 1, the deviation of the datum contributes to the overall error in stage 2. We extract from $\mathbf{x}_2$ the information on the features used as datum to form the vector $\mathbf{q}'$: The primary datum is the feature f_3 and the secondary and tertiary datum are the features f_1 and f_4, respectively. Therefore, we construct $\mathbf{q}' = [\mathbf{q}'^{\,T}_{\mathbf{f}_3}\ \ \mathbf{q}'^{\,T}_{\mathbf{f}_3}\ \ \mathbf{q}'^{\,T}_{\mathbf{f}_3}\ \ \mathbf{q}'^{\,T}_{\mathbf{f}_1}\ \ \mathbf{q}'^{\,T}_{\mathbf{f}_1}\ \ \mathbf{q}'^{\,T}_{\mathbf{f}_4}]^T$ with $\mathbf{q}'_{\mathbf{f}_1}$ known from stage 1 and $\mathbf{q}'_{\mathbf{f}_3} = \mathbf{q}'_{\mathbf{f}_4} = \mathbf{0}_{6\times1}$. We evaluate $\mathbf{F}_2$ using the nominal position of each feature, the nominal position of each locator in the PCS, and their associated norm given in Table II. After obtaining $\mathbf{F}_2$, shown in the second equation at the bottom of the page, the two sources of error can be combined together and the overall deviation of the PCS can be obtained as shown in Table IV. By following the procedure presented in Section II-B, the deviation $\mathbf{q}'_5$ of the new feature created at stage 2 can be calculated.

We have

$$
\mathbf{F}_3 = \begin{bmatrix} -0.2425 & 0 & 0.9701 & 0 & 30 & 0 \\ 0 & -1 & 0 & -104.2903 & 0 & 4.8507 \\ -0.9701 & 0 & -0.2425 & 0 & 100 & 0 \\ 0 & 0 & 0 & -0.2425 & 0 & 0.9701 \\ 0 & 0 & 0 & 0 & -1 & 0 \\ 0 & 0 & 0 & -0.9701 & -1 & -0.2425 \end{bmatrix}.
$$

Since the PCS is taken as the GCS, and since we still consider that there is no machining error, we have $\mathbf{F_4} = \mathbf{I}_{6\times6}$. We finally obtain $\mathbf{q}'_{\mathbf{f}_5}$ and update the state-space vector $\mathbf{x}_2$ into $\mathbf{x}_3 = [\mathbf{q}'^{\,T}_{\mathbf{f}_1}\ \ \mathbf{0}_{1\times6}\ \ \mathbf{0}_{1\times6}\ \ \mathbf{0}_{1\times6}\ \ \mathbf{q}'^{\,T}_{\mathbf{f}_5}]^T$.

$$
\mathbf{F}_1 = \begin{bmatrix}
-0.5547 & 0 & -0.83205 & 0 & 0 & 0 & 0 & 0 & 0 & 0 & 0 & 0 & 0 & 0 & 0 & 0 & 0 & 0 \\
0 & 0 & 0 & -0.5547 & 0 & -0.83205 & 0 & 0 & 0 & 0 & 0 & 0 & 0 & 0 & 0 & 0 & 0 & 0 \\
0 & 0 & 0 & 0 & 0 & 0 & -0.5547 & 0 & -0.83205 & 0 & 0 & 0 & 0 & 0 & 0 & 0 & 0 & 0 \\
0 & 0 & 0 & 0 & 0 & 0 & 0 & 0 & 0 & 0 & 1 & 0 & 0 & 0 & 0 & 0 & 0 & 0 \\
0 & 0 & 0 & 0 & 0 & 0 & 0 & 0 & 0 & 0 & 0 & 0 & 0 & 1 & 0 & 0 & 0 & 0 \\
0 & 0 & 0 & 0 & 0 & 0 & 0 & 0 & 0 & 0 & 0 & 0 & 0 & 0 & 0 & -1 & 0 & 0
\end{bmatrix}.
$$

$$
\mathbf{F}_2 = \left[\begin{matrix}
0.555 & 0 & 0.832 & 16.64 & 18.02 & -11.09 & 0 & 0 & 0 & 0 & 0 & 0 & 0 & 0 & 0 & 0 \\
0 & 0 & 0 & 0 & 0 & 0 & 0.555 & 0 & 0.832 & 49.92 & -18.03 & -33.28 & 0 & 0 & 0 & 0 \\
0 & 0 & 0 & 0 & 0 & 0 & 0 & 0 & 0 & 0 & 0 & 0 & 0.555 & 0 & 0.832 & 16.64 \\
0 & 0 & 0 & 0 & 0 & 0 & 0 & 0 & 0 & 0 & 0 & 0 & 0 & 0 & 0 & 0 \\
0 & 0 & 0 & 0 & 0 & 0 & 0 & 0 & 0 & 0 & 0 & 0 & 0 & 0 & 0 & 0 \\
0 & 0 & 0 & 0 & 0 & 0 & 0 & 0 & 0 & 0 & 0 & 0 & 0 & 0 & 0 & 0
\end{matrix}\right.
$$

$$
\left.\begin{matrix}
0 & 0 & 0 & 0 & 0 & 0 & 0 & 0 & 0 & 0 & 0 & 0 & 0 & 0 & 0 & 0 & 0 & 0 & 0 & 0 \\
0 & 0 & 0 & 0 & 0 & 0 & 0 & 0 & 0 & 0 & 0 & 0 & 0 & 0 & 0 & 0 & 0 & 0 & 0 & 0 \\
-72.11 & -11.09 & 0 & 0 & 0 & 0 & 0 & 0 & 0 & 0 & 0 & 0 & 0 & 0 & 0 & 0 & 0 & 0 & 0 & 0 \\
0 & 0 & 0 & 0 & -1 & -100 & -130 & 0 & 0 & 0 & 0 & 0 & 0 & 0 & 0 & 0 & 0 & 0 & 0 & 0 \\
0 & 0 & 0 & 0 & 0 & 0 & 0 & 0 & 0 & 0 & -1 & 0 & -70 & 0 & 0 & 0 & 0 & 0 & 0 & 0 \\
0 & 0 & 0 & 0 & 0 & 0 & 0 & 0 & 0 & 0 & 0 & 0 & 0 & 0 & 1 & 0 & 0 & 0 & -85 & -40
\end{matrix}\right]
$$

TABLE III
3DCS MODEL RESULTS ($\times 10^{-3}$)

		d_x	d_y	d_z	e_1	e_2	e_3
Stage 1	$\mathbf{q}_p(1)$	-400.55	62.57	285.23	-42.97	-308.54	-64.46
	$\mathbf{q}'_{\mathrm{f}_1}(1)$	400.68	446.53	-28.74	0.75	-1.12	5.38
Stage 2	$\mathbf{q}_p(2)$	5.13	-237.43	63.25	-42.97	-0.02	-64.46
	$\mathbf{q}'_{\mathrm{f}_5}(2)$	212.74	10.26	-216.94	-0.91	5.38	1.00

TABLE IV
ANALYTICAL MODEL RESULTS ($\times 10^{-3}$) AND THE RELATIVE DIFFERENCE FROM 3DCS RESULTS

		d_x	d_y	d_z	e_1	e_2	e_3
Stage 1	$\mathbf{q}_p(1)$	-402.69 (0.53%)	62.5 (0.11%)	285.13 (0.03%)	-42.97 (0.0%)	-308.52 (0.0%)	-64.46 (0.0%)
	$\mathbf{q}'_{\mathrm{f}_1}(1)$	402.69 (0.50%)	446.66 (0.02%)	-28.75 (0.03%)	0.75 (0.0%)	-1.12 (0.0%)	5.38 (0.0%)
Stage 2	$\mathbf{q}_p(2)$	5.10 (0.58%)	-237.50 (0.03%)	63.33 (0.13%)	-42.97 (0.0%)	0.00 (-)	-64.46 (0.0%)
	$\mathbf{q}'_{\mathrm{f}_5}(2)$	211.89 (0.39%)	10.25 (0.09%)	-216.51 (0.20%)	-0.91 (0.0%)	5.38 (0.0%)	1.00 (0.0%)

D. Validation of the Model Prediction

To validate the model, a machining model is developed using 3DCS software, which is widely used in industry for tolerancing management purposes. 3DCS software adopts the numerical simulation method for the prediction of process variation and no analytical model can be produced. Since 3DCS is standard industrial software, we can compare our model prediction with 3DCS's output to validate our results. In the 3DCS model, the same fixture error is intentionally added to the process at each stage.

The 3DCS model measurement results are listed in Table III. The measurement gives the deviation from nominal of both the PCS at each stage and the newly created feature with respect to the GCS. All of the measurements are in the global coordinate system taken as the PCS under nominal conditions. The model prediction for the comparison is listed in Table IV. For a plane feature, the relevant parameter is its orientation and the distance from the datum plane. The deviation of the orientation of a plane is denoted by $[e_1, e_2, e_3]$ and the deviation of the distance from the nominal plane is denoted by d_x, d_y, and d_z.

The comparison results indicate that the difference between the 3DCS prediction and the state transition model prediction are very small. The discrepancy is due to the linearization of the state transition model. The 3DCS results are from numerical calculations based on nonlinear relationships. The results show that the linearization error is quite small in this case: The study of the propagation of the linearization error in the multistage machining model would be interesting following the uncertainty analysis method developed by Shen [30]. These issues are now under investigation and will be reported in the near future.

IV. CONCLUSION

The complexity of a multistage machining process poses great challenges on root cause identification and process design evaluation. In this paper, an analytical linear model is developed to describe the propagation of workpiece geometric deviation among multiple machining stages. This linear model has a state-space form and the states are the workpiece geometric deviations. Using state transitions among multiple machining stages, this model describes the dimensional error accumulation and transformation when the workpiece passes through the whole process. A systematic procedure is presented to model the workpiece setup and cutting process in machining.

Although the developed linear model approximates the nonlinear relationship between process errors and product quality, the linearization-induced error has been shown to be ignorable under certain conditions (e.g., the case study presented in Section III). However, when the number of stages increases, the propagation of the linearization error warrants some rigorous investigation. This is our current research and the results will be reported in the near future.

This model has great potential to be applied to the root cause identification for purposes of quality improvement. For a complex machining process, it is often very difficult, if not impossible, to identify the faulty stage if certain features of the workpiece are out of specification. With this model which integrates process and product information, model-based fault diagnosis can be developed to quickly identify the faults. Although the model is limited to setup errors, its open structure provides a quantitative framework for further expansion. This model can be used for fixture design and optimization. This model provides a quantitative relationship between fixture locator errors and the geometric errors of the final workpiece. By considering this relationship, the fixture locator design can be evaluated and optimized. All of these potential works will be pursued and reported in the future.

APPENDIX

We provide the general expression of $\mathbf{F}_2$ in this appendix. If we define the following matrices:

$$\mathbf{E}_1 = \begin{bmatrix} 1 & 0 & 0 & 0 \\ 0 & 1 & 0 & 0 \\ 0 & 0 & 1 & 0 \end{bmatrix}, \quad \mathbf{E}_2 = \begin{bmatrix} 0 & 0 & 0 & 0 \\ 0 & 0 & -1 & 0 \\ 0 & 1 & 0 & 0 \\ 0 & 0 & 0 & 0 \end{bmatrix},$$

$$\mathbf{E}_3 = \begin{bmatrix} 0 & 0 & 1 & 0 \\ 0 & 0 & 0 & 0 \\ -1 & 0 & 0 & 0 \\ 0 & 0 & 0 & 0 \end{bmatrix} \quad \text{and} \quad \mathbf{E}_4 = \begin{bmatrix} 0 & -1 & 0 & 0 \\ 1 & 0 & 0 & 0 \\ 0 & 0 & 0 & 0 \\ 0 & 0 & 0 & 0 \end{bmatrix}$$

$$\mathbf{G}^1_{i,i_k} = \mathbf{n}'^{\,T}_{i_k} \cdot \mathbf{E}_1 \cdot {}^0\mathbf{H}'_i$$

$$\mathbf{G}^2_{i,i_k} = \mathbf{n}'^{\,T}_{i_k} \cdot \begin{bmatrix} [1 \;\; 0 \;\; 0 \;\; 0] \cdot {}^0\mathbf{H}'_i \cdot \mathbf{E}_2 \cdot \left({}^0\mathbf{H}'_i\right)^{-1} \\ [0 \;\; 1 \;\; 0 \;\; 0] \cdot {}^0\mathbf{H}'_i \cdot \mathbf{E}_2 \cdot \left({}^0\mathbf{H}'_i\right)^{-1} \\ [0 \;\; 0 \;\; 1 \;\; 0] \cdot {}^0\mathbf{H}'_i \cdot \mathbf{E}_2 \cdot \left({}^0\mathbf{H}'_i\right)^{-1} \end{bmatrix} \cdot \begin{bmatrix} {}^0\mathbf{t}'_{i_k} \\ 1 \end{bmatrix}$$

$$\mathbf{G}^3_{i,i_k} = \mathbf{n}'^{\,T}_{i_k} \cdot \begin{bmatrix} [1 \;\; 0 \;\; 0 \;\; 0] \cdot {}^0\mathbf{H}'_i \cdot \mathbf{E}_3 \cdot \left({}^0\mathbf{H}'_i\right)^{-1} \\ [0 \;\; 1 \;\; 0 \;\; 0] \cdot {}^0\mathbf{H}'_i \cdot \mathbf{E}_3 \cdot \left({}^0\mathbf{H}'_i\right)^{-1} \\ [0 \;\; 0 \;\; 1 \;\; 0] \cdot {}^0\mathbf{H}'_i \cdot \mathbf{E}_3 \cdot \left({}^0\mathbf{H}'_i\right)^{-1} \end{bmatrix} \cdot \begin{bmatrix} {}^0\mathbf{t}'_{i_k} \\ 1 \end{bmatrix}$$

$$\mathbf{G}^4_{i,i_k} = \mathbf{n}'^{\,T}_{i_k} \cdot \begin{bmatrix} [1 \;\; 0 \;\; 0 \;\; 0] \cdot {}^0\mathbf{H}'_i \cdot \mathbf{E}_4 \cdot \left({}^0\mathbf{H}'_i\right)^{-1} \\ [0 \;\; 1 \;\; 0 \;\; 0] \cdot {}^0\mathbf{H}'_i \cdot \mathbf{E}_4 \cdot \left({}^0\mathbf{H}'_i\right)^{-1} \\ [0 \;\; 0 \;\; 1 \;\; 0] \cdot {}^0\mathbf{H}'_i \cdot \mathbf{E}_4 \cdot \left({}^0\mathbf{H}'_i\right)^{-1} \end{bmatrix} \cdot \begin{bmatrix} {}^0\mathbf{t}'_{i_k} \\ 1 \end{bmatrix}$$

$$\mathbf{F}_2=\begin{bmatrix} \mathbf{G}^1_{i,i_1}\cdot\begin{bmatrix}1\\0\\0\\0\end{bmatrix}\mathbf{G}^1_{i,i_1}\cdot\begin{bmatrix}0\\1\\0\\0\end{bmatrix}\mathbf{G}^1_{i,i_1}\cdot\begin{bmatrix}0\\0\\1\\0\end{bmatrix}\mathbf{G}^2_{i,i_1}\ \mathbf{G}^3_{i,i_1}\ \mathbf{G}^4_{i,i_1} & & \mathbf{0}\\ & \ddots & \\ \mathbf{0} & & \mathbf{G}^1_{i,i_m}\cdot\begin{bmatrix}1\\0\\0\\0\end{bmatrix}\mathbf{G}^1_{i,i_m}\cdot\begin{bmatrix}0\\1\\0\\0\end{bmatrix}\mathbf{G}^1_{i,i_m}\cdot\begin{bmatrix}0\\0\\1\\0\end{bmatrix}\mathbf{G}^2_{i,i_m}\ \mathbf{G}^3_{i,i_m}\ \mathbf{G}^4_{i,i_m}\end{bmatrix}$$

then $\mathbf{F}_2$ can be expressed explicitly as shown in the equation at the top of the page.

ACKNOWLEDGMENT

The authors would like to thank R. Kumar, Dr. Y. Zhou, and J. Kong from Dimensional Control Systems, Inc., for their fruitful discussions. The authors also thank the editor and the referees for their valuable comments and suggestions.

REFERENCES

[1] D. Ceglarek and J. Shi, "Dimensional variation reduction for automotive body assembly," *Manufact. Rev.*, vol. 8, no. 1, pp. 139–154, 2004.

[2] D. Ceglarek, W. Huang, S. Zhou, Y. Ding, R. Kumar, and Y. Zhou, "Time-based competition in manufacturing: stream-of-variation analysis (SOVA) methodology—review," *Int. J. Flex. Manufact. Syst.*, vol. 16, no. 1, pp. 11–44, 2004.

[3] B. W. Shiu, D. Ceglarek, and J. Shi, "Multi-stations sheet metal assembly modeling and diagnostics," *Trans. NAMRI*, vol. 24, pp. 199–204, 1996.

[4] V. B. Kreng, C. R. Liu, and C. N. Chu, "A kinematic model for machine tool accuracy characterization," *Int. J. Adv. Manufact. Technol.*, vol. 9, pp. 79–86, 1994.

[5] E. S. Lee, S. H. Suh, and J. W. Shon, "A comprehensive method for calibration of volumetric positioning accuracy of CNC-machines," *Int. J. Adv. Manufact. Technol.*, vol. 14, pp. 43–49, 1998.

[6] G. Chen, J. Yuan, and J. Ni, "A displacement measurement approach for machine geometric error assessment," *Int. J. Mach. Tools Manufact.*, vol. 41, pp. 149–161, 2001.

[7] A. C. Okafor and Y. M. Ertekin, "Derivation of machine tool error models and error compensation procedure for three axes vertical machining center using rigid body kinematics," *Int. J. Mach. Tool Manufact.*, vol. 40, pp. 1199–1213, 2000.

[8] J. Ni and S. M. Wu, "An on-line measurement technique for machine volumetric error compensation," *ASME Trans., J. Eng. Ind.*, vol. 115, pp. 85–92, 1993.

[9] J. H. Lee and S. H. Yang, "Statistical optimization and assessment of a thermal error model for CNC machine tools," *Int. J. Mach. Tools Manufact.*, vol. 42, no. 1, pp. 147–155, 2002.

[10] C. D. Mize and J. C. Ziegert, "Neural network thermal error compensation of a machining center," *Precision Eng.*, vol. 24, no. 4, pp. 338–346, 2000.

[11] J. Yang, J. Yuan, and J. Ni, "Thermal error mode analysis and robust modeling for error compensation on a CNC turning center," *Int. J. Mach. Tools Manufact.*, vol. 39, no. 9, pp. 1367–1381, 1999.

[12] C. Lo, J. Yuan, and J. Ni, "Optimal temperature variable selection by grouping approach for thermal error modeling and compensation," *Int. J. Mach. Tools Manufact.*, vol. 39, no. 9, pp. 1383–1396, 1999.

[13] J. Fuh, C. Chang, and M. Melkanoff, "An integrated fixture planning and analysis system for machining processes," *Robot. Comput.-Integr. Manufact.*, vol. 10, no. 5, pp. 339–353, 1993.

[14] E. C. De Meter, "Min-max load model for optimizing machining fixture performance," *ASME Trans., J. Eng. Ind.*, vol. 117, pp. 186–193, 1995.

[15] Y. Rong and Y. Bai, "Machining accuracy analysis for computer-aided fixture design verification," *ASME Trans., J. Manufact. Sci. Eng.*, vol. 118, pp. 289–299, 1996.

[16] M. J. Hockenberger and E. C. De Meter, "The application of meta functions to the quasi-static analysis of workpiece displacement within a machining fixture," *ASME Trans., J. Manufact. Sci. Eng.*, vol. 118, pp. 325–331, 1996.

[17] J. Yang, J. Yuan, and J. Ni, "Real-time cutting force induced error compensation on a turning center," *Int. J. Mach. Tools Manufact.*, vol. 37, no. 11, pp. 1597–1610, 1997.

[18] S. G. Chen, A. G. Ulsoy, and Y. Koren, "Error source diagnostics using a turning process simulator," *ASME Trans., J. Manufact. Sci. Eng.*, vol. 120, pp. 409–416, 1998.

[19] J. R. Mayer, A. V. Phan, and G. Cloutier, "Prediction of diameter errors in bar turning: a computationally effective model," *Appl. Math. Model.*, vol. 24, pp. 943–956, 2000.

[20] J. F. Lawless, R. J. Mackay, and J. A. Robinson, "Analysis of variation transmission in manufacturing processes—Part I," *J. Qual. Technol.*, vol. 31, no. 2, pp. 131–142, 1999.

[21] R. Agrawal, J. F. Lawless, and R. J. Mackay, "Analysis of variation transmission in manufacturing processes—Part II," *J. Qual. Technol.*, vol. 31, no. 2, pp. 143–154, 1999.

[22] J. Jin and J. Shi, "State space modeling of sheet metal assembly for dimensional control," *J. Manufact. Sci. Eng.*, vol. 121, pp. 756–762, Nov. 1999.

[23] Y. Ding, D. Ceglarek, and J. Shi, "Modeling and diagnosis of multistage manufacturing processes: part I state space model," presented at the Proc. 2000 Japan/USA Symp. Flexible Automation, Ann Arbor, MI, Jul. 23–26, 2000, 2000JUSFA-13146.

[24] ——, "Fault diagnosis of multistage manufacturing processes by using state space approach," *ASME Trans., J. Manufact. Sci. Eng.*, vol. 124, no. 2, pp. 313–322, 2002.

[25] Q. Huang, N. Zhou, and J. Shi, "Stream of Variation Modeling and Diagnosis of Multi-Station Machining Processes," in *Proc. IMECE 2000*, Orlando, FL, Nov. 5–10, 2000, pp. 81–88, MED-Vol. 11.

[26] W. Zhong, Y. Huang, and S. J. Hu, "Modeling variation propagation in machining systems with different configurations," in *Proc. ASME MECE*, New Orleans, LA, Nov. 2002, pp. 97–106.

[27] D. Djurdjanovic and J. Ni, "Linear state space modeling of dimensional machining errors," *Trans. NAMRI/SME*, vol. 29, pp. 541–548, 2001.

[28] S. Zhou, Q. Huang, and J. Shi, "State space modeling of dimensional variation propagation in multistage machining process using differential motion vectors," *IEEE Trans. Robot. Autom.*, vol. 19, no. 2, pp. 296–309, Apr. 2003.

[29] Y. Rong, S. H. Huang, and Z. Hou, *Advanced Computer-Aided Fixture Design*. Boston, MA: Elsevier, 2005, 414 p..

[30] Y. Shen and N. A. Duffie, "An uncertainty analysis method for coordinate referencing in manufacturing systems," *Trans. ASME, J. Eng. Ind.*, vol. 117, pp. 42–48, 1995.

[31] J. J. Craig, *Introduction to Robotics*. Reading, MA: Addison-Wesley, 1988.

[32] R. P. Paul, *Robot Manipulators: Mathematics, Programming, and Control*. Cambridge, MA: MIT, 1981.

[33] G. Henzold, *Handbook of Geometrical Tolerancing: Design, Manufacturing and Inspection*. New York: Wiley, 1995.

[34] H. Z. Yau, "Evaluation and uncertainty analysis of vectorial tolerances," *Precision Eng.*, vol. 20, pp. 123–137, 1997.

[35] W. Cai, J. Hu, and J. Yuan, "A variational method of robust fixture configuration design for 3-D workpieces," *J. Manufact. Sci. Eng.*, vol. 119, pp. 593–602, Nov. 1997.

Jean-Philippe Loose received the B.S. degree in industrial engineering from the ENSIACET engineering school of France in 2004 and the M.S. degree in industrial engineering from the University of Wisconsin, Madison, in 2004, and is currently pursuing the Ph.D. degree in industrial engineering at the University of Wisconsin, Madison.

Mr. Loose is a member of the Society of Mechanical Engineers (SME) and Institute of Operations Research and Management Sciences (INFORMS).

Shiyu Zhou received the B.S. and M.S. degrees in mechanical engineering from the University of Science and Technology, Heifei, China, in 1993 and 1996, respectively, and the M.Sc. degree in industrial engineering and Ph.D. degree in mechanical engineering from the University of Michigan, Ann Arbor, in 2000.

Currently, he is an Assistant Professor in the Department of Industrial and Systems Engineering at the University of Wisconsin-Madison. His research interests are the in-process quality and productivity improvement methodologies by integrating statistics, system and control theory, and engineering knowledge. The objective is to achieve automatic process monitoring, diagnosis, compensation, and their implementation in various manufacturing processes.

Dr. Zhou is a recipient of the CAREER Award from the National Science Foundation in 2006. Dr. Zhou is a member of the Institute of Industrial Engineers (IIE), Institute of Operations Research and Management Sciences (INFORMS), American Association of Mechanical Engineers (ASME), and the Society of Mechanical Engineers (SME).

Dariusz Ceglarek (M'03) received the Ph.D. degree in mechanical engineering from the University of Michigan, Ann Arbor, in 1994.

He was on the research faculty at the University of Michigan, Ann Arbor, from 1995 to 2000. In 2000, he moved to the University of Wisconsin, Madison, as Assistant Professor in the Department of Industrial and Systems Engineering where he rose to the rank of Associate Professor and Professor in 2003 and 2005, respectively. Previously, he was Chair of the Quality, Statistics and Reliability Section of the Institute of Operations Research and Management Sciences (INFORMS). Currently, he is a Program Chair for the Amercian Association of Mechanical Engineers (ASME) Design-for-Manufacturing Life Cycle (DFMLC) Conferences, Corresponding Member of CIRP (International Institution for Production Engineering Research), based in Paris, France, and serves as Associate Editor of the *ASME Transactions, Journal of Manufacturing Science and Engineering*. He is also on the program review panel for the State of Louisiana Board of Regents R&D Program. His research focuses on the integration of design and manufacturing in product life cycle with an emphasis on multistage production systems convertibility, scalability, and diagnosability as well as on product quality and service. He has developed a number of methodologies for ramp-up time and variation reduction; optimal sensing networks in manufacturing; and reconfigurable/reusable assembly systems.

Dr. Ceglarek has received numerous awards including the National Science Foundation (NSF) CAREER Award; 1998 Dell K. Allen Outstanding Young Manufacturing Engineer of the Year Award from the Society of Manufacturing Engineers (SME); 1999 Outstanding Research Scientist Award from the College of Engineering; University of Michigan, and three Best Paper Awards by ASME Manufacturing Engineering Division, ASME Design Engineering Division, and the Best Application Paper Award by the Institute of Industrial Engineers (IIE) *Transactions on Quality and Reliability Engineering.*